Supplement of Atmos. Chem. Phys., 24, 13065–13079, 2024
https://doi.org/10.5194/acp-24-13065-2024-supplement

Atmospheric Chemistry and Physics
Open Access

Supplement of

Enhanced daytime secondary aerosol formation driven by gas–particle partitioning in downwind urban plumes

Mingfu Cai et al.

Correspondence to: Bin Yuan (byuan@jnu.edu.cn)

Table S1. Fitting parameters a and b of different calibration experiments.

Experiment No.	Particle diameter (nm)	Mass loading (ng)	a	b
1	200	150.7	-0.197	1.056
2	200	241	-0.167	1.768
3	200	407	-0.206	3.732
4	100	90.5	-0.218	3.641
5	100	110.6	-0.241	5.229
6	100	150.8	-0.243	4.451

Table S2. The detailed information of three selected periods.

	Periods	Days
Long-range Transport	14-20 October; 29 October-1 November; 3-4 November; 7-10 November; 14 November	18
Urban Air Masses	7-9 October; 23-27 October; 1-2 November; 13 November	11
Coastal Air Masses	2-4 October; 10-12 October; 22 October; 12 November	8

Figure S1. Location of the measurement site and Guangzhou city. This map was obtained from Map World (www.tianditu.gov.cn).

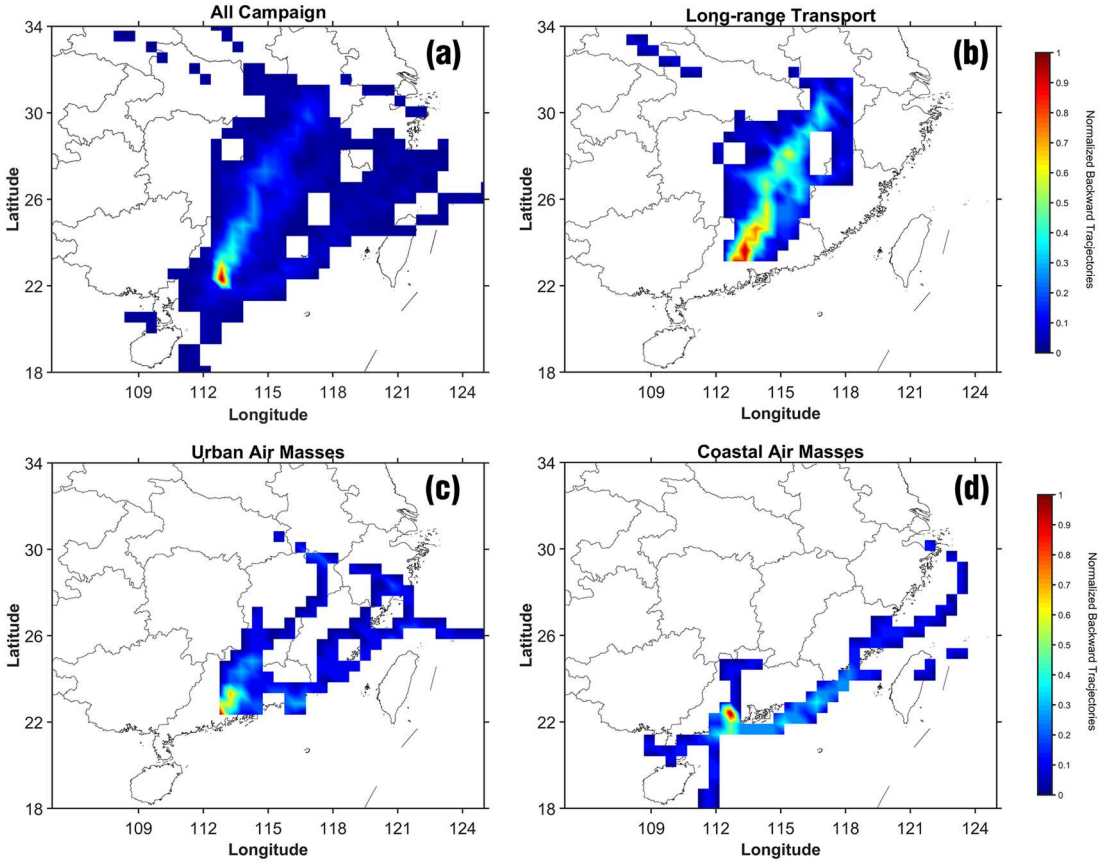

Figure S2. Normalized 72 hours backward trajectories arriving at the measurement site during (a) the whole measurement, (b) long-range transport period, (c) urban air masses period, and (d) coastal air masses period.

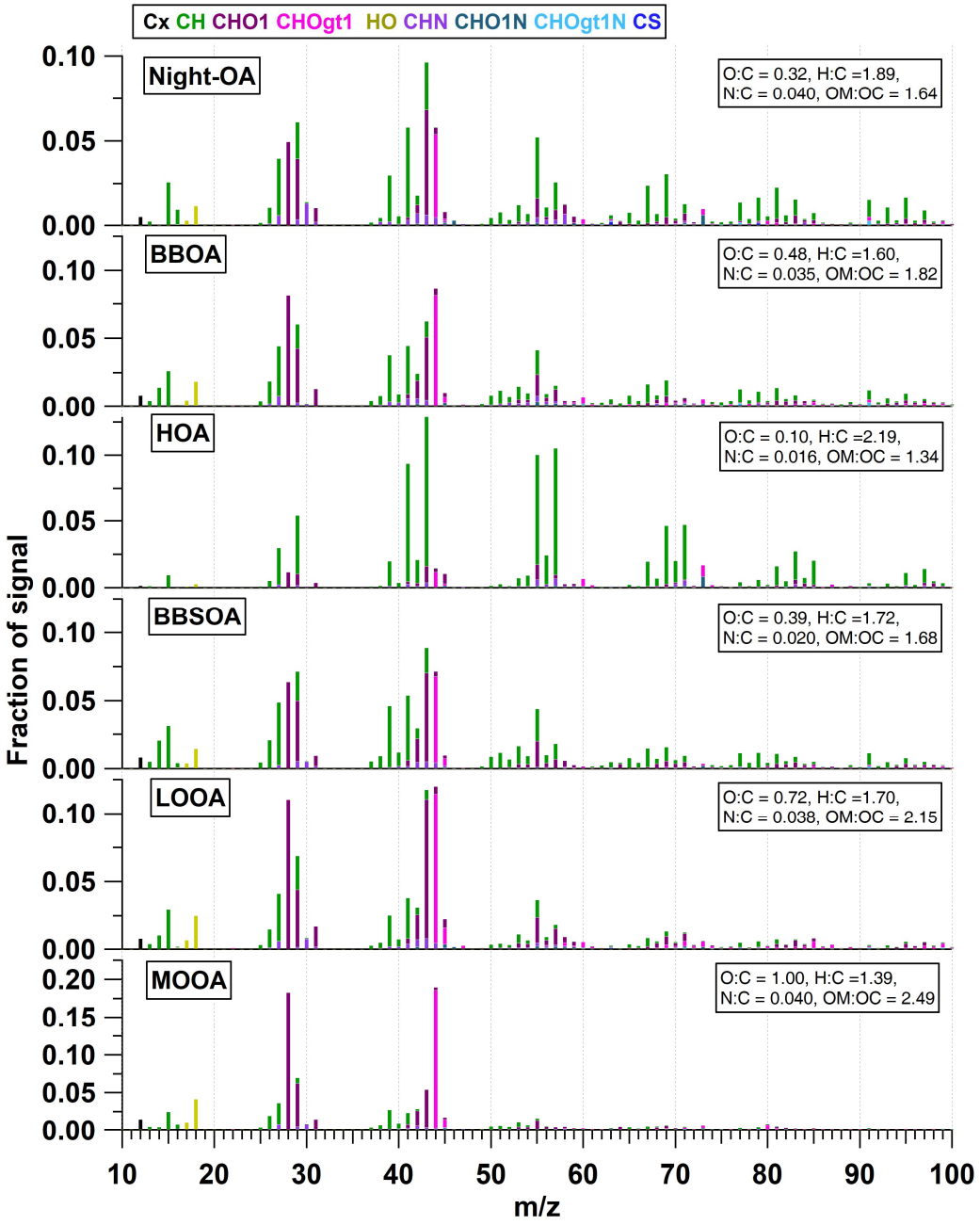

Figure S3. Mass spectral profile of six OA factors. The colors represent different family groups.

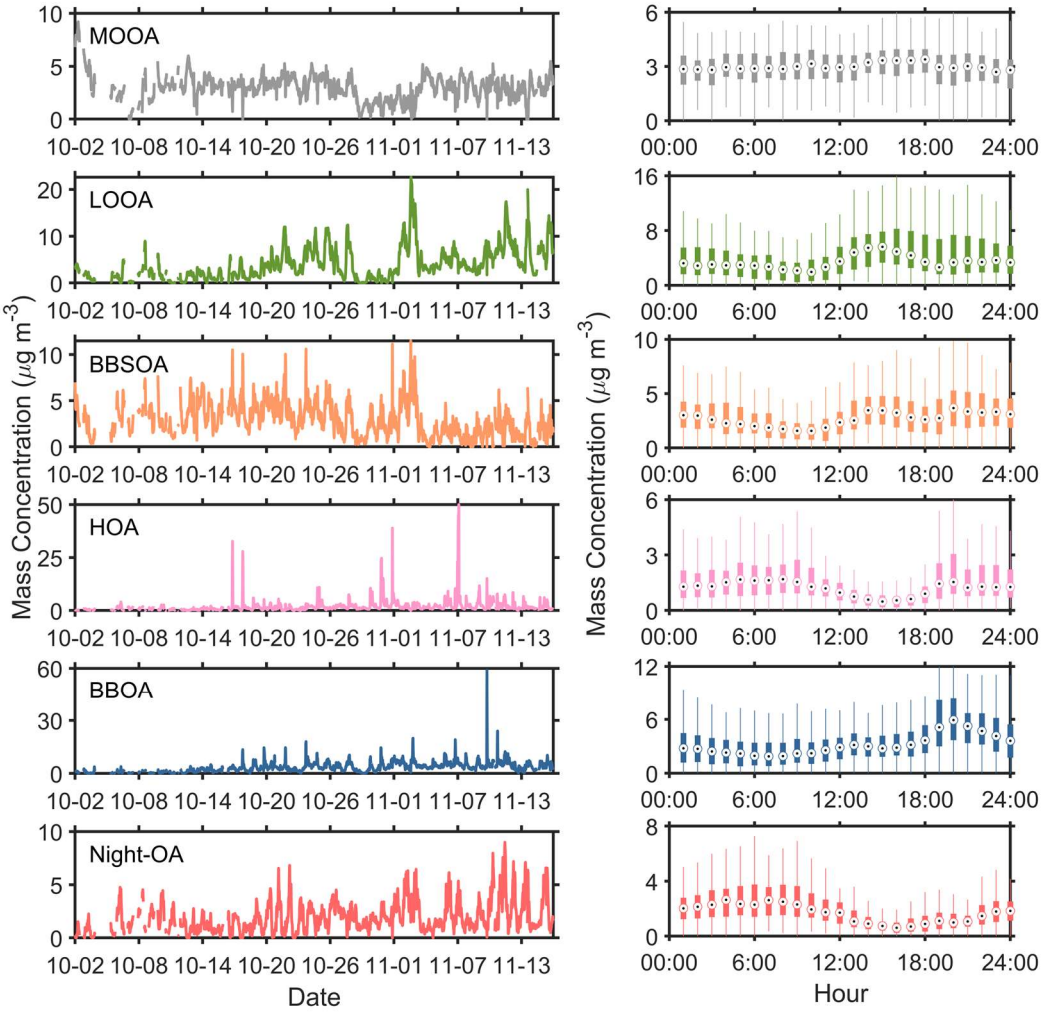

Figure S4. Timeseries and diurnal variation of six OA factors.

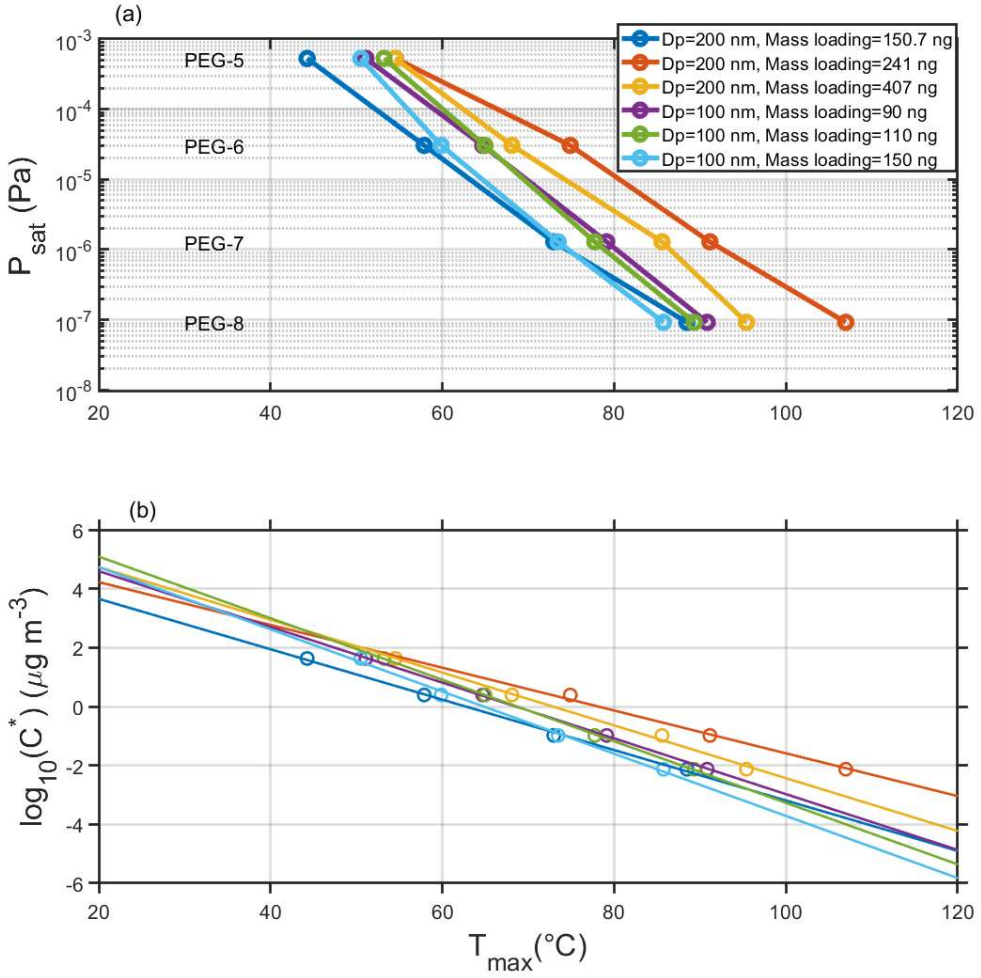

Figure S5. (a) Measured T_{max} vs P_{sat} literature values for PEG 5-8 at different diameters and collected mass loadings and (b) corresponding fitted calibration lines.

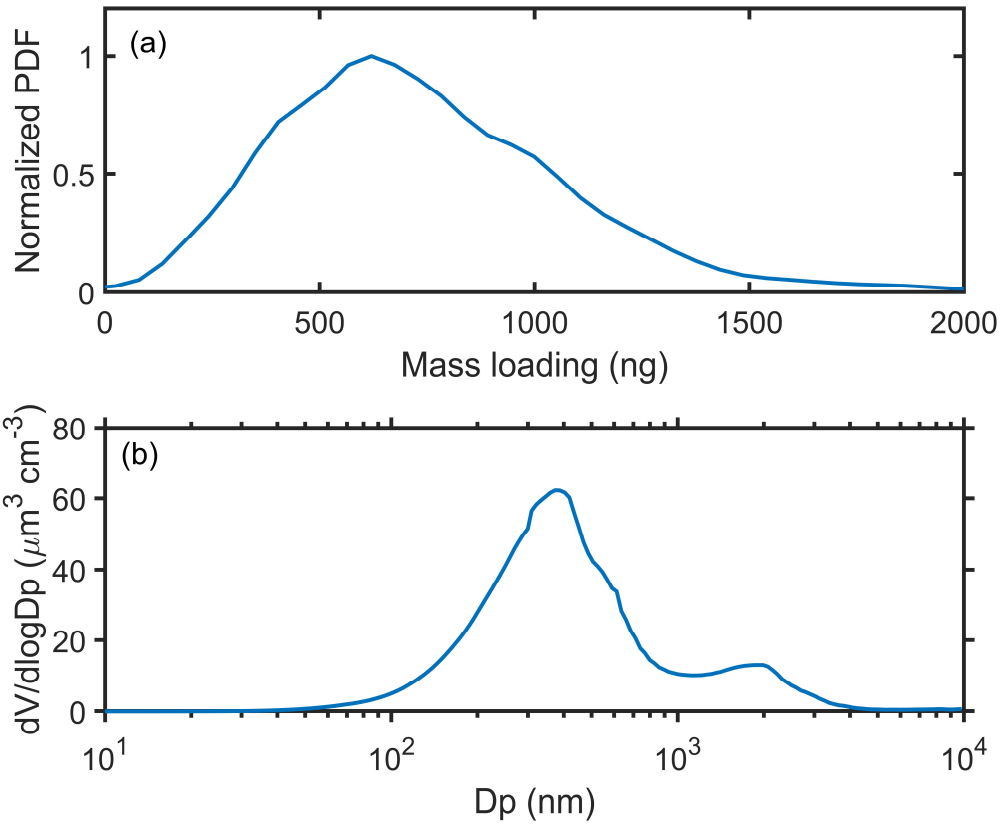

Figure S6. (a) Normalized probability density function of collected mass loading on the filter of the FIGAERO-I-CIMS and (b) the average particle volume size distribution. The collected mass loading is calculated based on collection time, flow rate through the filter, and the organic concentration measured by the SP-AMS.

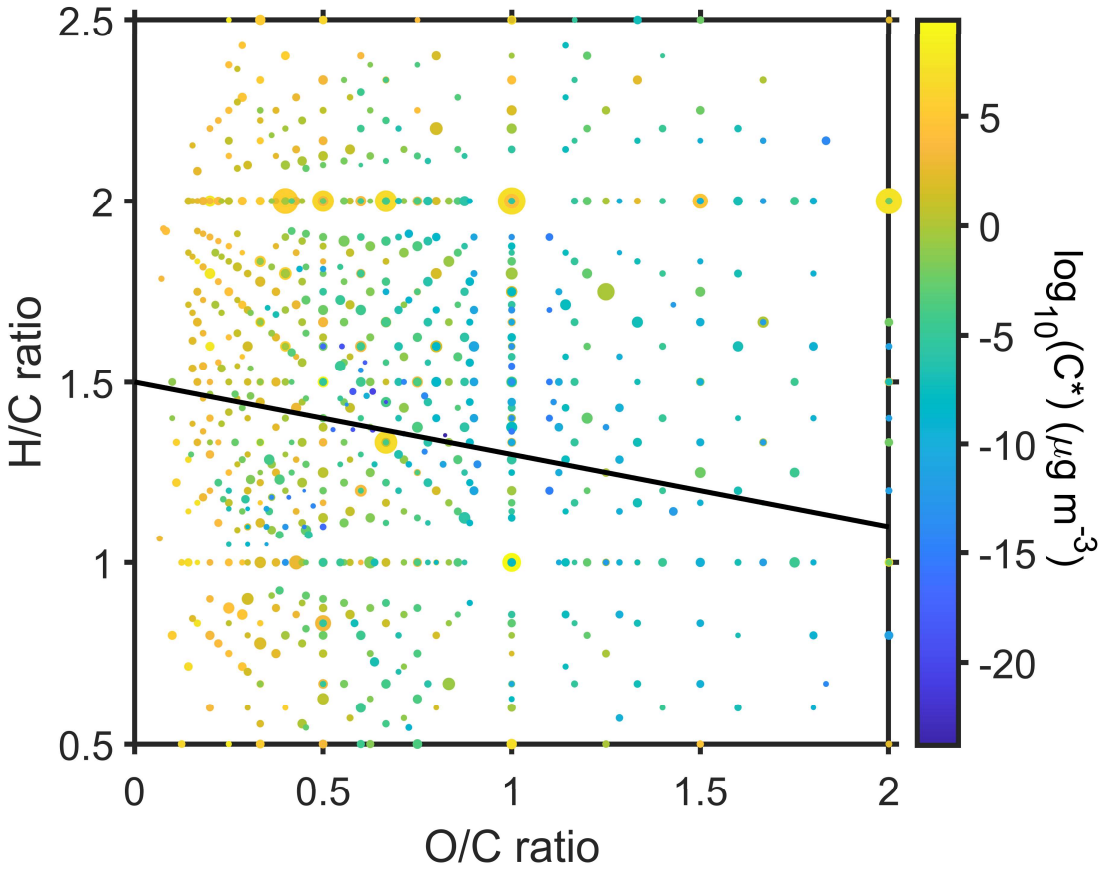

Figure S7. Van-Krevelen diagram (O/C ratio versus H/C ratio) of gas-phase organic compounds measured by FIGAERO-CIMS. The symbol size is proportional to the mass concentration of organic vapors and the color code represents the volatility. The black solid line divided the organic vapors potentially formed through the autoxidation pathway (upper regime) and multi-generation OH oxidation pathway (lower regime), based on the oxidation products aromatics and monoterpene, respectively (Wang et al., 2022; Wang et al., 2020).

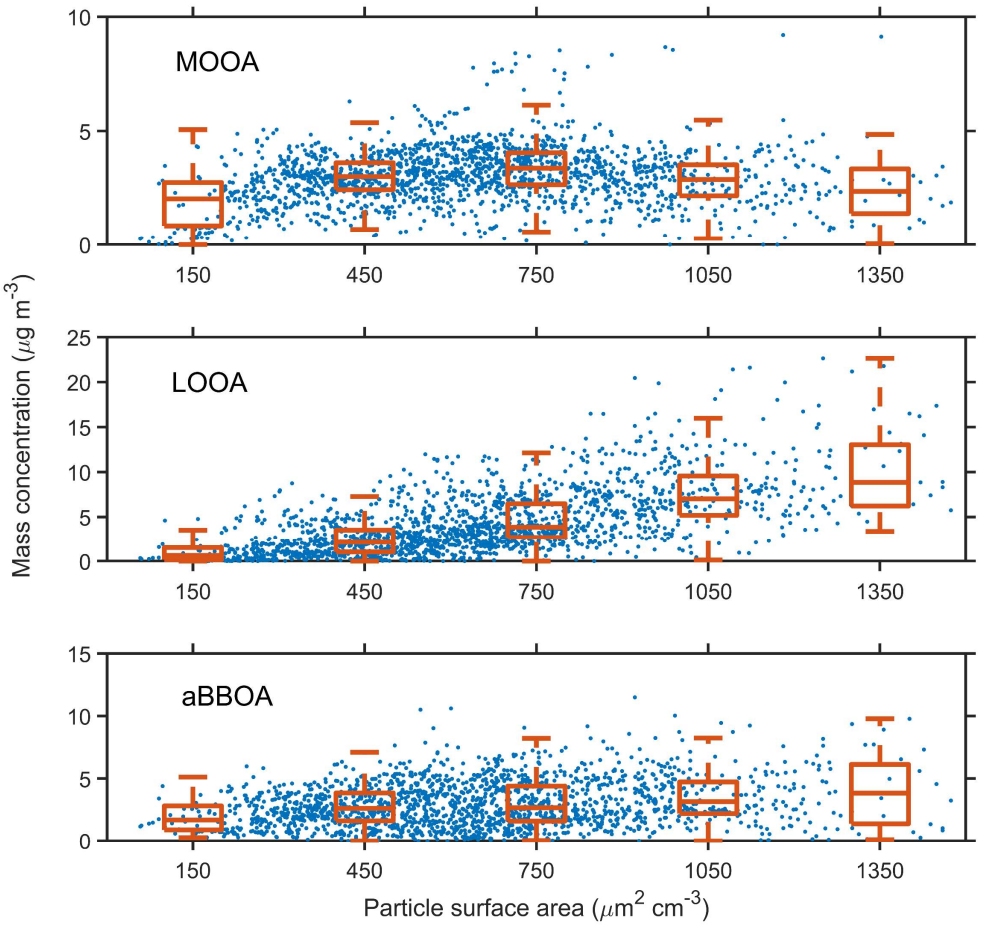

Figure S8. Relationship between particle surface area and SOA factors (MOOA, LOOA and aBBOA).

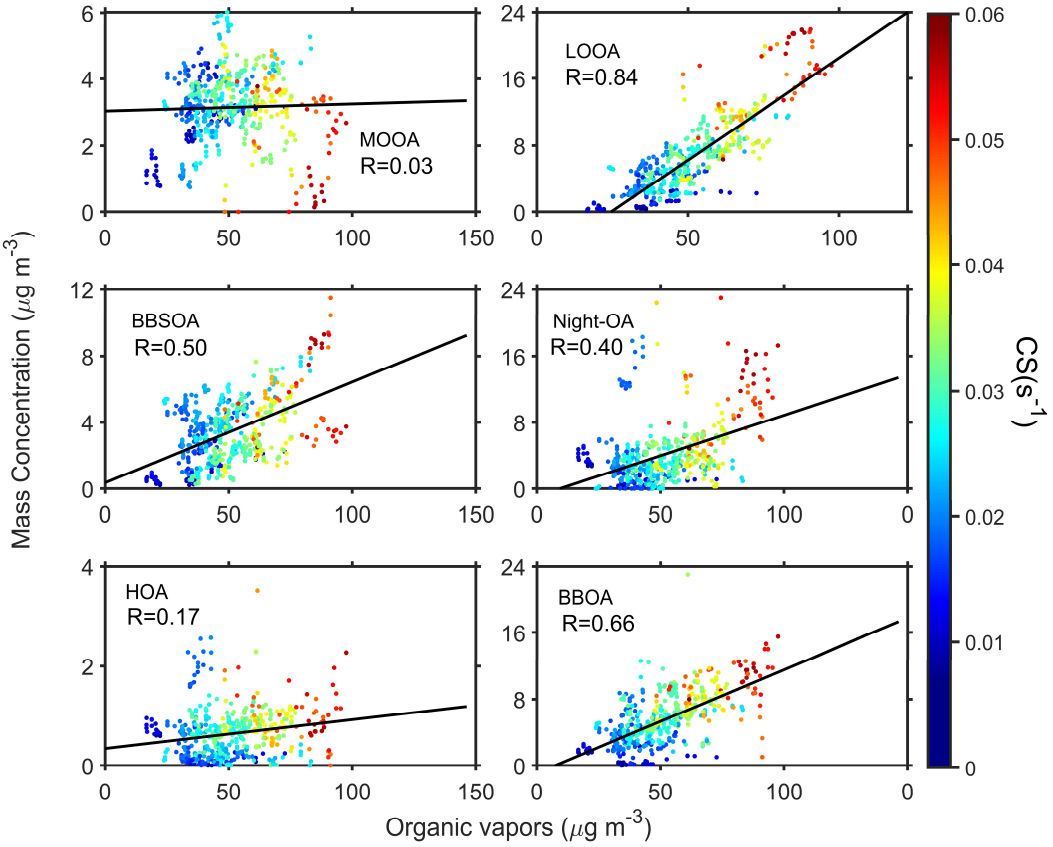

Figure S9. Relationship between the concentration of organic vapors and six OA PMF factors. The color represents the CS values.

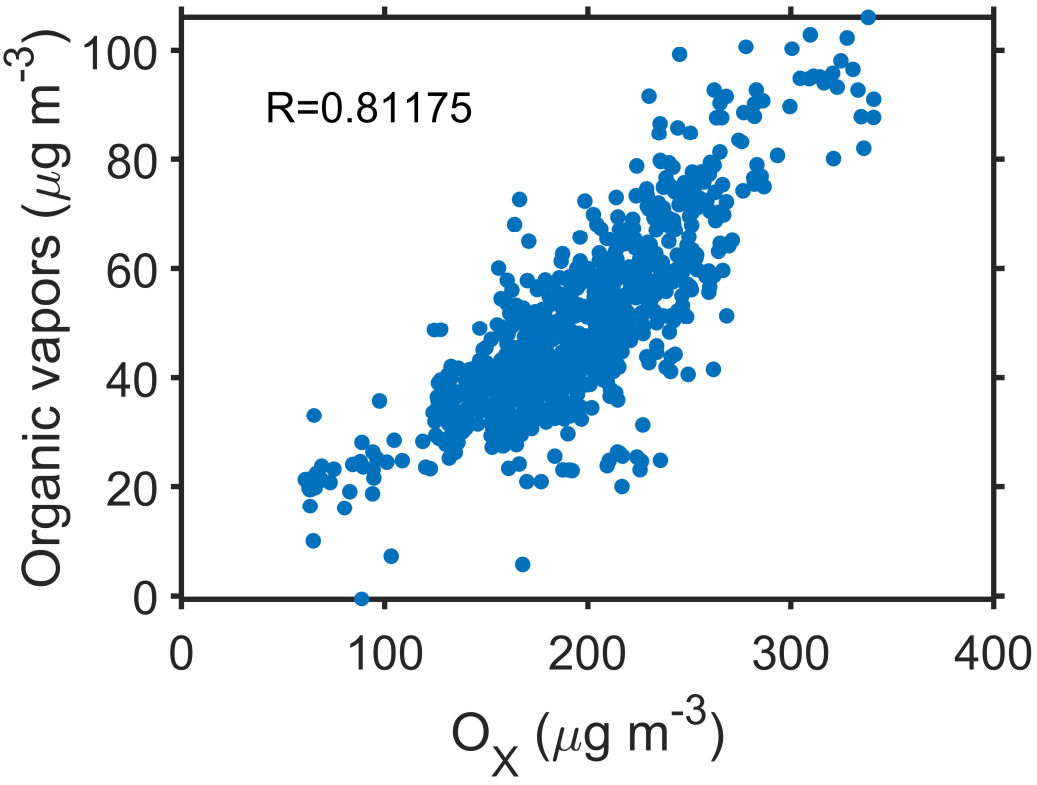

Figure S10. Relationship between odd-oxygen (O_X, O_X=O_3+NO_2) and the concentration of organic vapors measured by the FIGAERO-CIMS in the afternoon (10:00-16:00 LT).

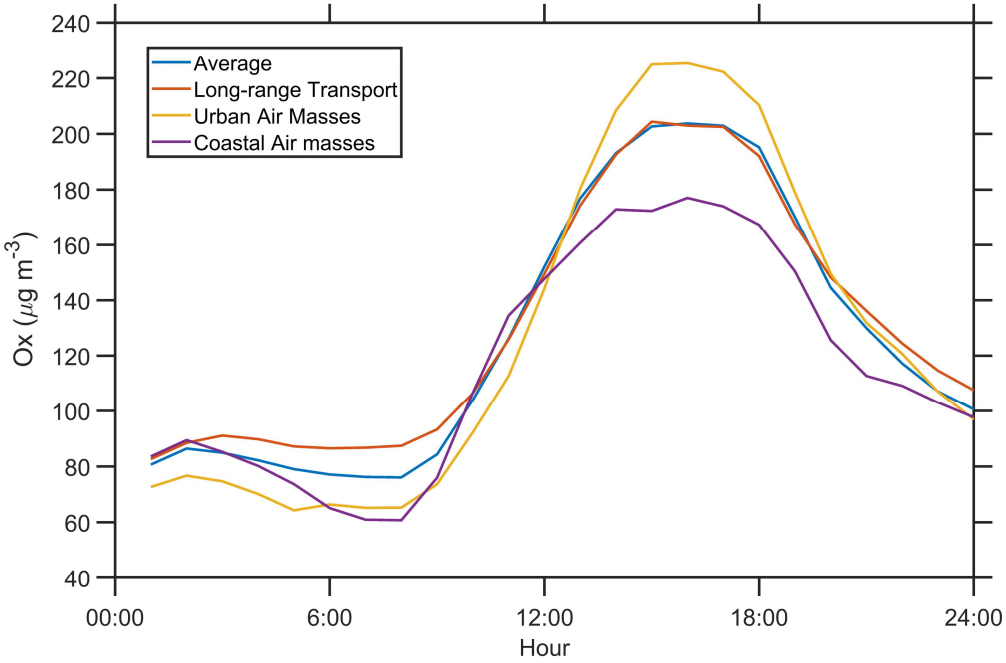

Figure S11. The average diurnal variation of O_x during the whole campaign, long-range transport, urban air masses, and coastal air masses periods.

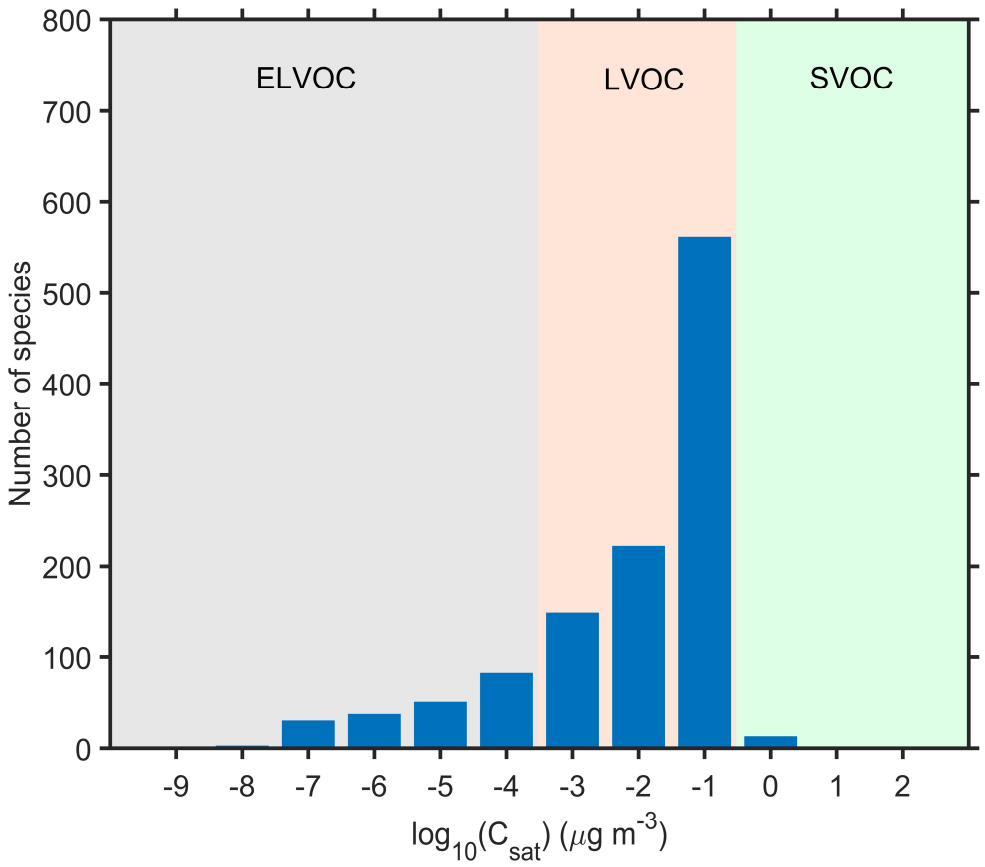

Figure S12. Volatility distribution of the number of calibrated and semi-quantified species measured by the FIGAERO-CIMS.

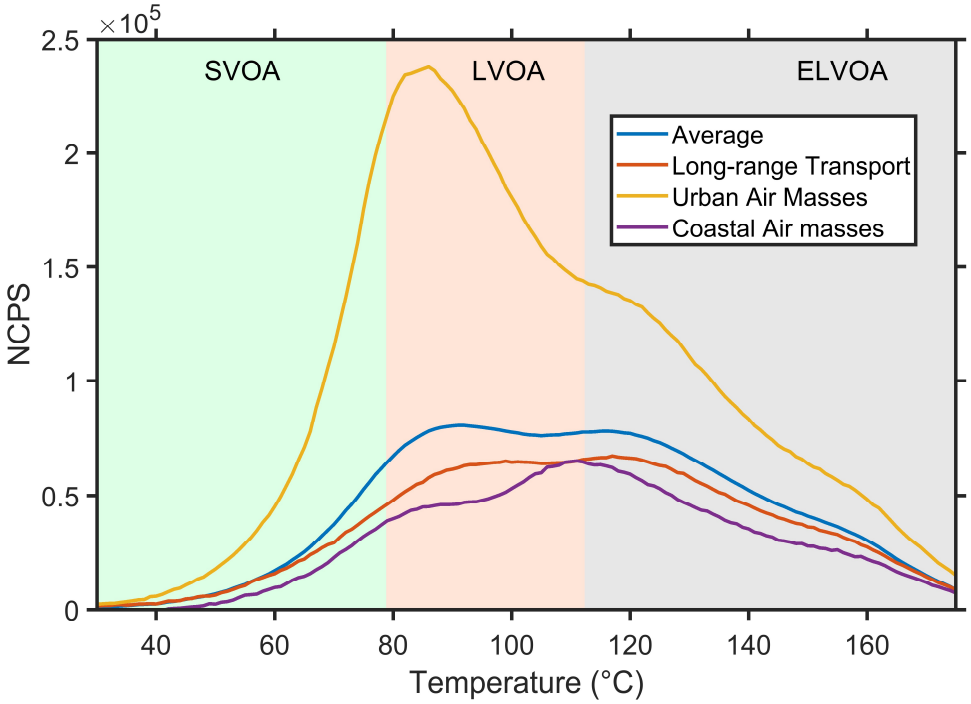

Figure S13. Average sum thermograms measured by the FIGAERO-CIMS in the afternoon (12:00-16:00 LT) during the whole campaign, long-range transport, urban air masses, and coastal air masses periods.

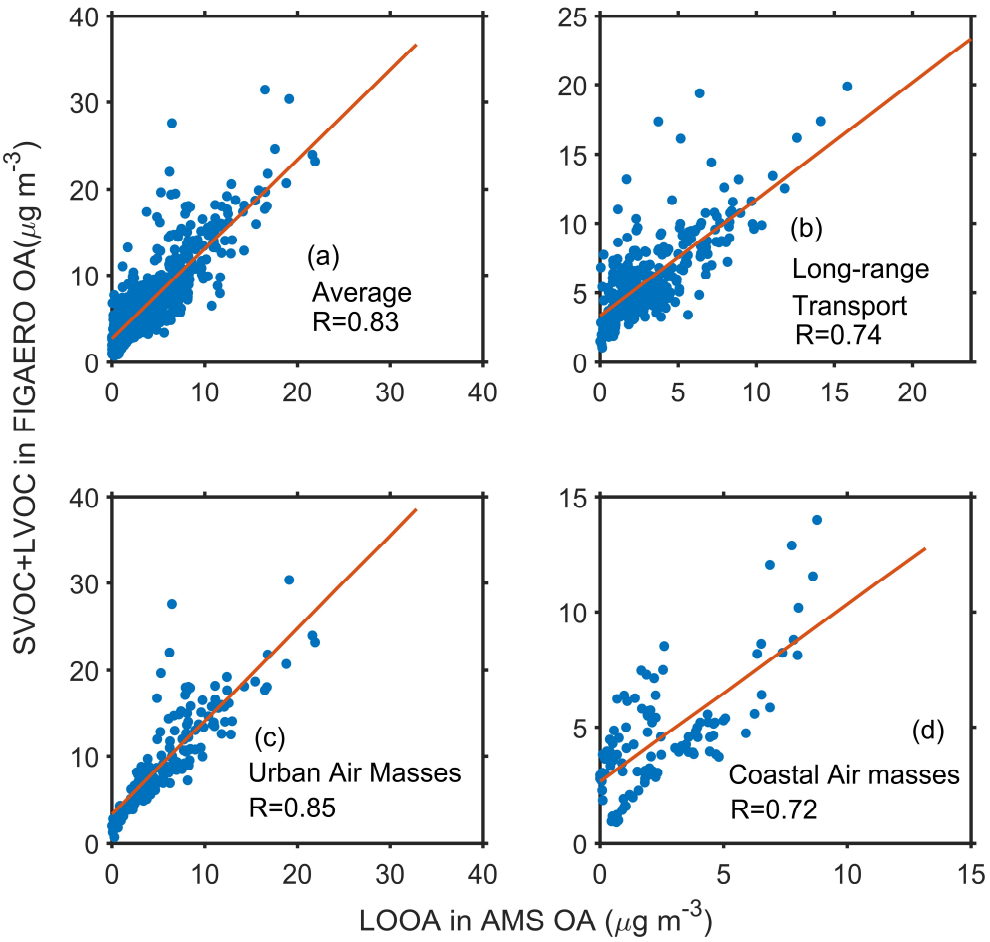

Figure S14. Relationship between the SVOC+LVOC in FIGAERO OA and LOOA in AMS OA during (a) the whole campaign, (b) long-range transport, (c) urban air masses, and (d) coastal air masses periods.

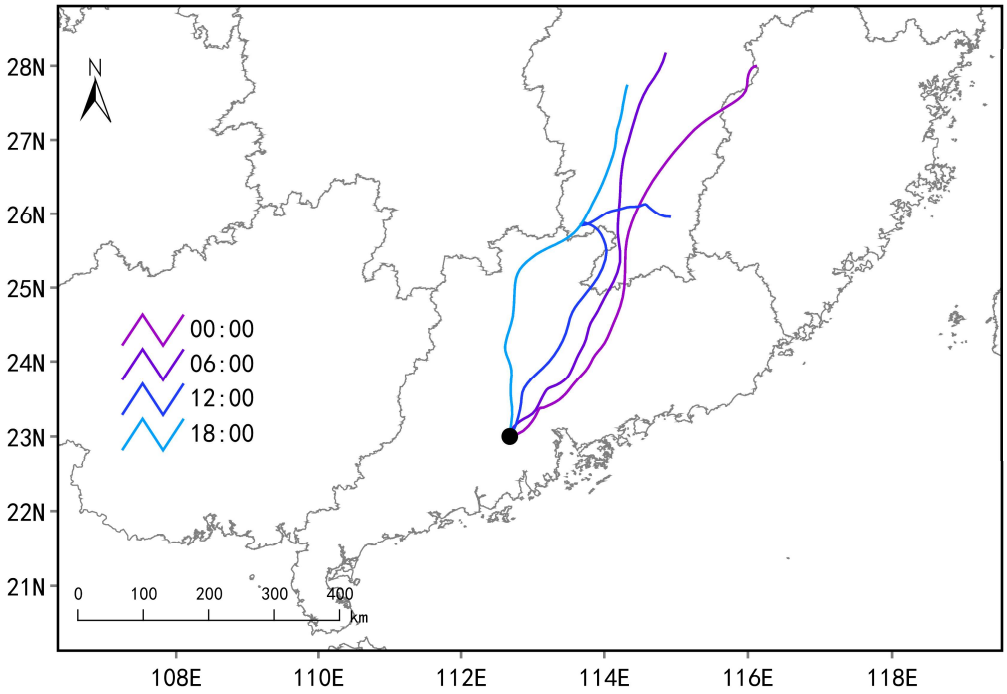

Figure S15. 72h backward trajectories arriving at the measurement site with 500 m height at 00:00, 06:00, 12:00, and 18:00 on 2 November 2019.

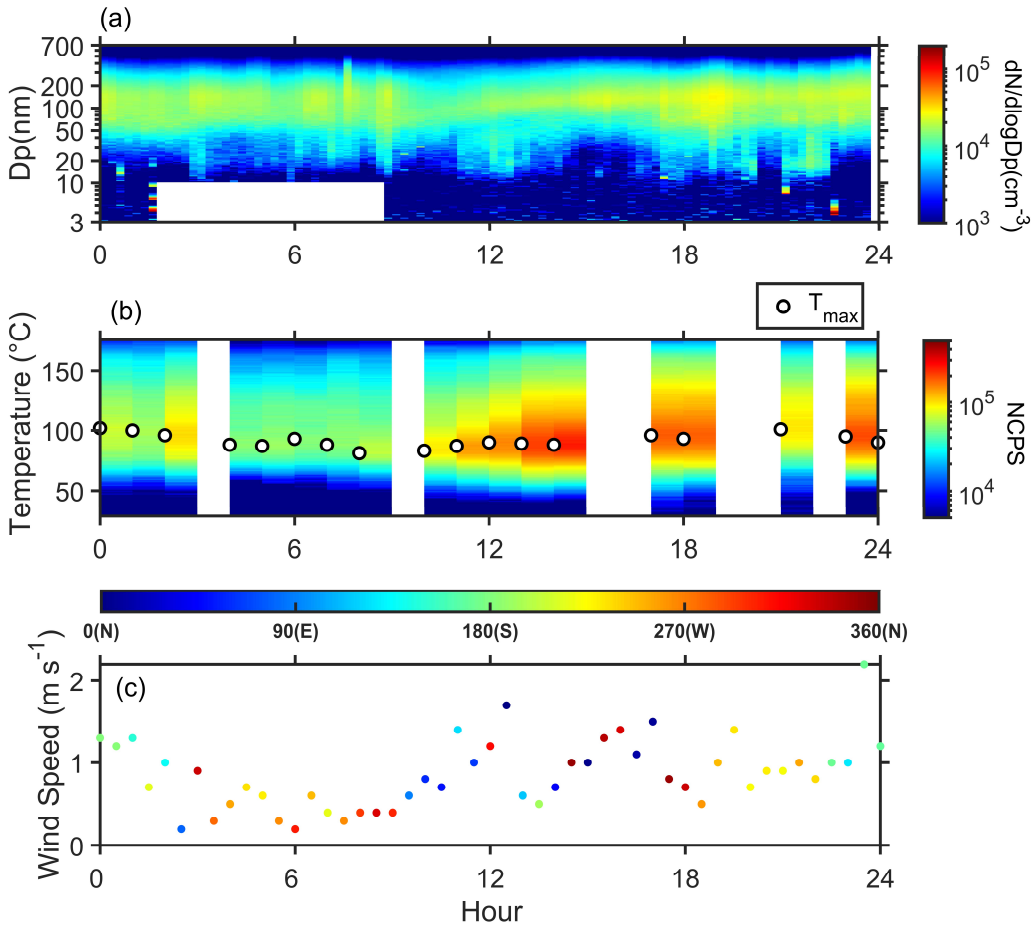

Figure S16. Variation of (a) PNSD, (b) sum thermograms, and (c) wind speed and direction on 2 November 2019.

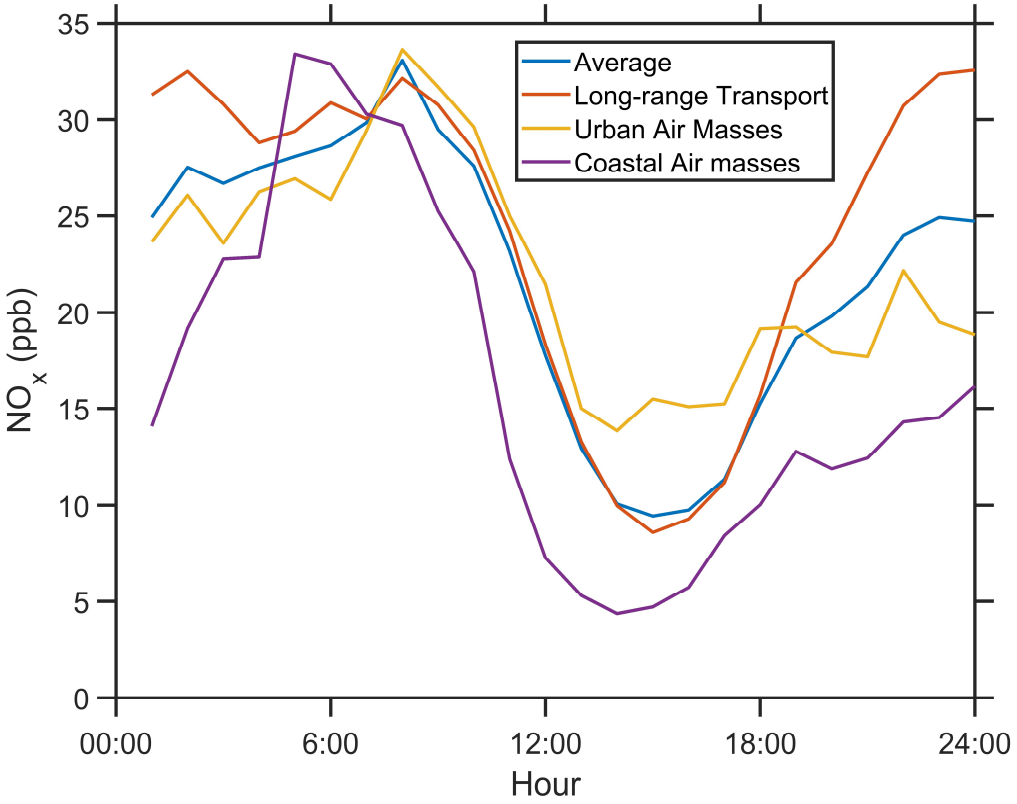

Figure S17. The average diurnal variation of NO_x during the whole campaign and three selected periods.

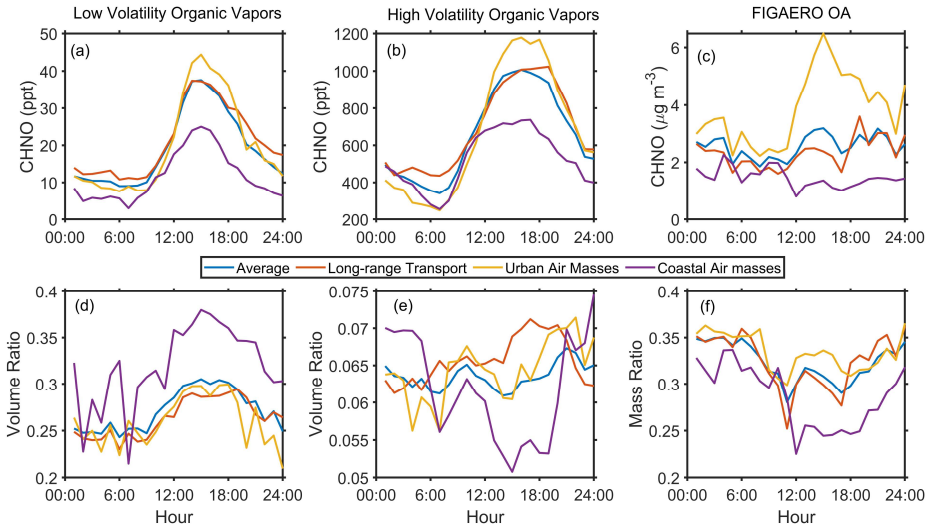

Figure S18. Diurnal variation of CHON compounds in (a) low volatility organic vapors, (b) high volatility organic vapors, and (c) FIGAERO OA and (d-f) their corresponding mass ratio.

References

Nie, W., Yan, C., Huang, D. D., Wang, Z., Liu, Y., Qiao, X., Guo, Y., Tian, L., Zheng, P., Xu, Z., Li, Y., Xu, Z., Qi, X., Sun, P., Wang, J., Zheng, F., Li, X., Yin, R., Dallenbach, K. R., Bianchi, F., Petäjä, T., Zhang, Y., Wang, M., Schervish, M., Wang, S., Qiao, L., Wang, Q., Zhou, M., Wang, H., Yu, C., Yao, D., Guo, H., Ye, P., Lee, S., Li, Y. J., Liu, Y., Chi, X., Kerminen, V.-M., Ehn, M., Donahue, N. M., Wang, T., Huang, C., Kulmala, M., Worsnop, D., Jiang, J., and Ding, A.: Secondary organic aerosol formed by condensing anthropogenic vapours over China's megacities, Nature Geoscience, 10.1038/s41561-022-00922-5, 2022.

Wang, M., Chen, D., Xiao, M., Ye, Q., Stolzenburg, D., Hofbauer, V., Ye, P., Vogel, A. L., Mauldin, R. L., Amorim, A., Baccarini, A., Baumgartner, B., Brilke, S., Dada, L., Dias, A., Duplissy, J., Finkenzeller, H., Garmash, O., He, X.-C., Hoyle, C. R., Kim, C., Kvashnin, A., Lehtipalo, K., Fischer, L., Molteni, U., Petäjä, T., Pospisilova, V., Quéléver, L. L. J., Rissanen, M., Simon, M., Tauber, C., Tomé, A., Wagner, A. C., Weitz, L., Volkamer, R., Winkler, P. M., Kirkby, J., Worsnop, D. R., Kulmala, M., Baltensperger, U., Dommen, J., El-Haddad, I., and Donahue, N. M.: Photo-oxidation of Aromatic Hydrocarbons Produces Low-Volatility Organic Compounds, Environmental Science & Technology, 54, 7911-7921, 10.1021/acs.est.0c02100, 2020.

Wang, Y., Clusius, P., Yan, C., Dällenbach, K., Yin, R., Wang, M., He, X.-C., Chu, B., Lu, Y., Dada, L., Kangasluoma, J., Rantala, P., Deng, C., Lin, Z., Wang, W., Yao, L., Fan, X., Du, W., Cai, J., Heikkinen, L., Tham, Y. J., Zha, Q., Ling, Z., Junninen, H., Petäjä, T., Ge, M., Wang, Y., He, H., Worsnop, D. R., Kerminen, V.-M., Bianchi, F., Wang, L., Jiang, J., Liu, Y., Boy, M., Ehn, M., Donahue, N. M., and Kulmala, M.: Molecular Composition of Oxygenated Organic Molecules and Their Contributions to Organic Aerosol in Beijing, Environmental Science & Technology, 56, 770-778, 10.1021/acs.est.1c05191, 2022.